

UC Santa Barbara

UC Santa Barbara Previously Published Works

Title

Schmitt trigger using a self-healing ionic liquid gated transistor

Permalink

<https://escholarship.org/uc/item/3ms32281>

Journal

Advanced Materials, 27(21)

ISSN

0935-9648

Authors

Bubel, S
Menyo, MS
Mates, TE
[et al.](#)

Publication Date

2015-06-01

DOI

10.1002/adma.201500556

Peer reviewed

Schmitt Trigger Using a Self-Healing Ionic Liquid Gated Transistor

Simon Bubel, Matthew S. Menyo, Thomas E. Mates, J. Herbert Waite,
and Michael L. Chabinye*

Living organisms use self-assembled structures that rely on controlling ions to form sensors and collect, process, and transmit information without using large scale integrated semi-conducting circuits.^[1] Developing electronic devices inspired by such strategies, i.e., ion motion and electrochemical reactions, can lead to novel functionality. We show here how coupling of electrical and electrochemical properties can be designed to reproduce the characteristics of a Schmitt trigger in a single element. The Schmitt trigger is a circuit used for noise filtering and analog-to-digital converters,^[2] and it can be used as a basic element of neuromorphic electronic systems.^[3,4] To form a simple Schmitt trigger in one device element, we couple electrochemical reactions of an ionic liquid gated metal oxide semiconductor and a common biomolecule to provide stable operation through a chemical mechanism. This coupling is a type of a chemical self-healing mechanism because of its reversibility, and we expect that such a mechanism can also be extended to other materials as well. We believe that new devices that use ion kinetics inspired by living organisms may lead to highly integrated electronic circuits for smart sensor and ubiquitous computing applications.^[5]

Electrochemistry is used in a wide range of electronic devices, such as batteries,^[6] super capacitors,^[7] dye sensitized solar cells,^[8] electrochromic glasses, and mechanical actuators.^[9] There has been much attention recently to ionic devices. For example, ionic currents in electrolytes can be used directly to achieve rectification^[10] or switching^[11] of electric currents. Ionic liquids have been used as “gates” in field effect devices for switching, memory applications, and the study of fundamental transport properties.^[12–17]

The electric double layer (EDL) formed by the application of a voltage to an ionic liquid provides the means to accumulate or deplete charge at an interface with a semiconductor. In EDL-based devices, the surface of a functional material is exposed to relatively aggressive electrochemical environment.^[18] As such,

EDL devices can show noisy operation and may not tolerate long periods of electrical stress due to electrochemical reactions without exact compliance within the operating voltages.^[5,19–21] It is, therefore, important to determine the limits of their performance and to determine if there are new opportunities presented by the electrochemical reactivity. Indeed, there have already been significant advances in coupling ionic motion in the solid state to achieve novel electronic devices, such as memristors and synaptic transistors.^[22,23]

An intriguing goal for biomimetic circuits is to achieve low power consumption through simple design. To accomplish such functionality, novel devices should combine complex response in a single building block. Here, we present a hybrid device that combines a solid state material and a liquid interface that connects ion kinetics and electrochemistry beneficially. This four terminal device has a comparator characteristic exhibiting a memory free hysteresis that only depends on the direction of the voltage sweep, much like a Schmitt trigger, but with reduced complexity and power consumption. Such building blocks can be used as analog-to-digital converters^[24] and in circuits for neural networks.^[3]

It is known that when using ionic liquids to electrostatically gate metal oxide surfaces,^[13,21] electrochemical reactions can complicate their operation.^[5,19–21] These apparent non-idealities are associated with the formation and fate of oxygen ions and radicals. For example, a metal oxide surface exhibits corner atoms and absorbed water that can exchange oxygen at the interface with the ionic liquid. In addition, the ionic liquid itself may contain atmospheric oxygen and water as impurities (even at small levels in the best systems).^[25] The general solution to achieve stable operation is to reduce the maximum applied bias voltage to well below the expected onset of degradation,^[26,27] or to use a less reactive ionic liquid.^[15,25,28] To achieve stable electrical operation that does not require precise control of the applied bias, a solution is to develop a mechanism to heal the interface by employing a reaction path that is kinetically competitive with the degradation process.

As a model system, we use amorphous zinc oxide (*a*-ZnO) formed by a low temperature solution growth process that can lead to stable device operation in EDL transistor (EDLT) within a gate bias range below 4 V.^[29] Here, we modify the growth process to form a less stable, oxygen deficient *a*-ZnO thin film (Figure 1). We grew pinhole free films of *a*-ZnO that were 5 nm thick for the EDLT devices (physical characterization of the films provided in the Supporting Information, Figure S1) and characterized them under a nitrogen atmosphere. The films made for this study are relatively unstable in an EDLT using [EMIM][TCB] (1-ethyl-3-methylimidazolium tetracyanoborate), as demonstrated by changes in the onset voltage and

Dr. S. Bubel, Dr. T. E. Mates, Prof. M. L. Chabinye
Materials Research Laboratory (MRL)
University of California
Santa Barbara, CA 93106, USA
E-mail: mchabinye@engineering.ucsb.edu

Dr. M. S. Menyo, Prof. J. H. Waite
Biomolecular Science and Engineering
University of California
Santa Barbara, CA 93106, USA

Dr. M. S. Menyo, Prof. J. H. Waite
Molecular, Cell and Developmental Biology
University of California
Santa Barbara, CA 93106, USA



DOI: 10.1002/adma.201500556

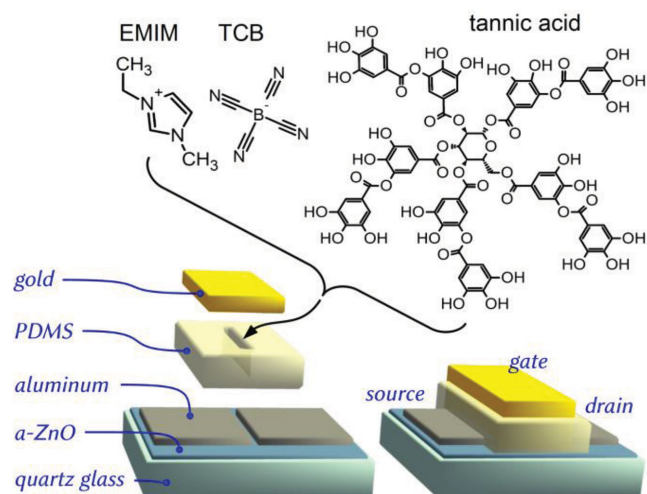


Figure 1. Layout of the field effect device and chemical structure of ionic liquid and polyphenol. [EMIM][TCB]: Cation and anion of the electrolyte, *a*-ZnO: solution processed amorphous zinc oxide, PDMS: stick-on cavity.

on/off ratio during repeated biasing (electrical characteristics of EDLTs and [EMIM][TCB] are given in Supporting Information, Figures S2–S6). The reported electrochemical window of [EMIM][TCB] against glassy carbon or silver chloride is ≈ 4.6 – 5.0 V.^[25,30,31] The degradation of *a*-ZnO, i.e., etching, is based on the cathodic reduction of the thin film and the production of oxygen species such as superoxide,^[32] which, in turn, are known to degrade the electrolyte and the electrodes eventually. These secondary reactions prevent the reversible redox cycle in *a*-ZnO EDLTs and are responsible for the degradation of EDLT characteristics. However, due to the small contact area of 0.012 cm² to very thin *a*-ZnO, the production of superoxide is limited and no visible secondary reactions such as leaching of the gold electrode or clouding of the ionic liquid can be observed.

To form stable EDLTs, we formed devices that included a kinetically competitive mechanism to the electrochemical degradation of *a*-ZnO. A biocompatible scavenger of reactive oxygen species is tannic acid, which is also known to bind to many inorganic surfaces.^[33–36] Tannic acid is an oxygen scavenger that can trap radicals species and, at the same time, acts as a source of oxygen to heal the highly conductive, reduced *a*-ZnO surface. A voltammetry measurement of an Al|*a*-ZnO|electrolyte|Au cell (Supporting Information, Figure S4) shows that the addition of tannic acid reduces the current density at biases exceeding 2.5 V, while it also introduces partial reversibility of the reaction (shown with an additional peak in the reverse bias sweep direction). By dissolving this polyphenol into the ionic liquid (Figure 1), we

obtain stable EDLT operation in a wide bias range that exceeds 7 V (± 3.5 V) at room temperature (Figure 2a) and therewith extends the bias window relative to devices without additives. While other EDLT systems have shown nearly comparable electrochemical windows,^[15,16,28] our results specifically demonstrate how an unstable system can be made stable with a simple chemical change.

The stabilizing effect of tannic acid can be seen by comparison of current–voltage characteristics after repeated biasing. The transfer characteristic in Figure 2a shows the tannic acid EDLT exhibiting an onset voltage of -0.6 V that is stable upon repeated operation in all bias ranges from 3 to 7 V. For the measurement, repetitive transfer characteristics were recorded with the gate bias spanning over an increasing voltage range (Supporting Information, Figure S2). The hysteresis proved to be reproducible (Figure 2a), and the maximum current and on/off ratio can be seen to be independent of the applied bias ranges up to driving conditions over 7 V (Supporting Information, Figure S2). In contrast, a device with pure ionic liquid [EMIM][TCB] exhibits an unstable onset voltage that increases as the device is operated at higher gate voltages or biased repetitively. Without the additive the EDLT exhibits the behavior of a degenerately doped semiconductor with an onset voltage of -1.5 V, far in the negative regime. Increasing the applied gate voltage range to 7 V successively increases the onset voltage to nearly $+1$ V and degrades the maximum current, irreversibly (Supporting Information, Figure S2).

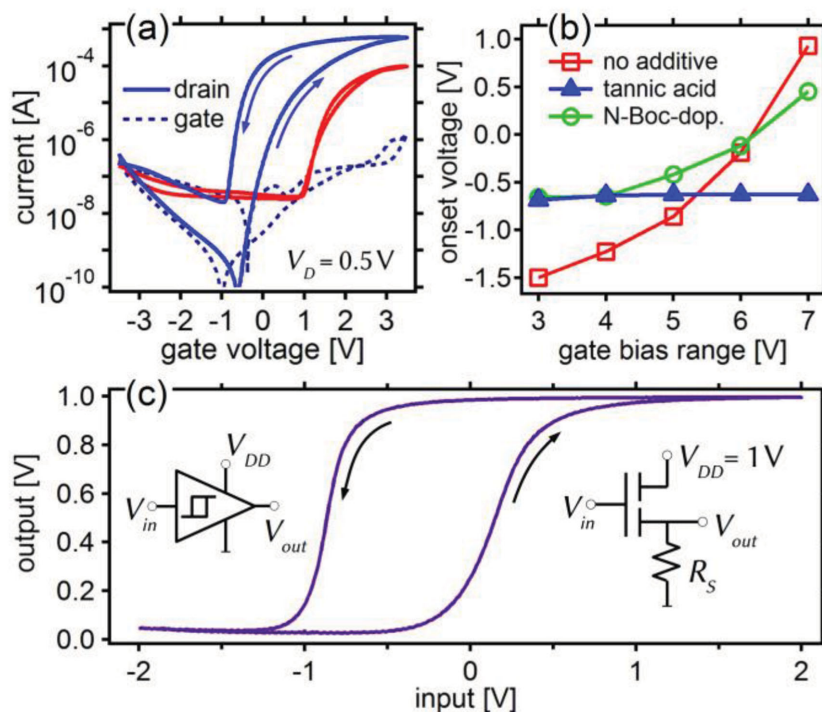


Figure 2. Properties of IL-gated TFTs and Schmitt trigger circuit. a) Transfer characteristic of hysteretic EDLT with [EMIM][TCB] at 0.1 V s⁻¹ with tannic acid (blue line, broken line for gate current) and without tannic acid (red line). b) Onset voltage of EDLTs dependent on the applied gate bias range during transfer measurements. c) Output characteristic of the circuit employing the hysteretic EDLT at 0.1 V s⁻¹. Insets: symbol of the Schmitt trigger (left) and equivalent circuit (right).

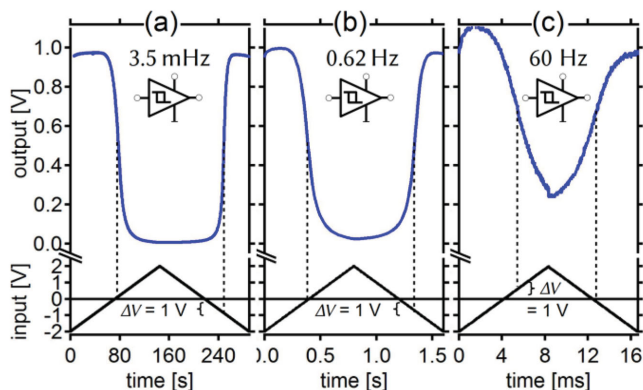


Figure 3. Inverting Schmitt trigger output characteristic for saw tooth input signal. Supply voltage $V_{DD} = 1$ V. a) Driving frequency of 2.8 mHz. b) 0.62 Hz. c) 60 Hz. ΔV describes the hysteresis that can be used for noise permissive switching.

The surprising stabilizing effect of the tannic acid additive provides a new functionality: by the addition of a resistor, either at the source or at the drain side, a simple comparator with a memory-free hysteresis resembling a Schmitt trigger can be built. The output characteristic and circuitry with a source resistor of 800 k Ω are shown in Figure 2c. The device exhibits a hysteresis of 1 V and switches between 0 and the supply voltage around an input signal of -0.5 V. **Figure 3** shows the output voltage of the inverting Schmitt trigger employing a 250 k Ω drain resistor. When operated at different driving frequencies between 3.5 mHz and 60 Hz, the Schmitt trigger switches with a stable hysteresis of 1 V and clearly defined on and off states. At higher frequencies, and due to the large device structure and the limited speed of the kinetic system, the voltage of the gate capacitor that becomes alternately charged with ± 2 V is superimposed on the output signal. This parasitic voltage results in an output voltage that exceeds the supply voltage by 10% and produces increasing deviation from unity voltage gain at higher frequencies. In contrast to other reports on electrochemical devices,^[22] these Schmitt triggers do not show a persistent memory effect and were operational at frequencies exceeding 100 Hz without noticeable degradation for more than a month (Supporting Information, Figures S7 and S8).

The stabilization of the device relies on the electrochemical reaction of the metal oxide and the additive. ZnO and its amorphous thin films, in particular, possess very diverse intrinsic doping mechanisms that can be influenced by the surface chemistry and the oxygen stoichiometry of the film. In general, an oxygen deficient film is more conductive than a stoichiometric film.^[21] In the case of surface passivation however, the conductivity depends on the dipole moment of the adsorbate. For example, alkyl- and aryl-carboxylic and phosphonic acids are known to promote the surface conductivity of crystalline ZnO, while hydroxide and water coordination leads to the formation of an insulating surface region.^[37,38]

The influence of the additives can be seen in the transfer characteristics of the devices in Figure 2b. Here, a negative onset voltage means that the film is conductive at zero gate bias. Comparing the trend in onset voltage at gate bias ranges below 5 V, the first difference that stands out when adding

oxygen scavengers is the change in conductivity. Much like in many other reports,^[25,37] the here used *a*-ZnO surface is oxygen deficient, i.e., possesses a conducting surface. We found that the degenerate behavior of the *a*-ZnO surface is removed by molecules with catechol or gallic acid groups (Supporting Information, Figure S3). These polyphenols are known to coordinate at unsaturated surface cations.^[35,36,39,40] With *N*-Boc-dopamine (*tert*-butyl [*N*-2-(3,4-hydroxyphenyl)ethyl]carbamate) the transistor onset voltages, shown in Figure 2b, demonstrate that effect for smaller bias ranges up to 4 V. The same initial stabilization can be seen when tannic acid is used as an additive, and X-ray photoelectron spectroscopy (XPS) measurements show the coverage with tannic acid regardless of the applied bias (Supporting Information, Figure S11). Despite the oxygen radical scavenging properties of both additives, *N*-Boc-dopamine does not stabilize the oxide film and the application of bias voltage range ≥ 5 V results in a shift of the onset voltage from -0.6 to $+0.5$ V.

We can understand the origin of the difference in the behavior of the EDL devices by considering the chemical differences of *N*-Boc-dopamine and tannic acid. Both have catechol functionalities that link to the metal oxide surface and both are also present within the bulk solution. A key difference is that tannic acid is a multifunctional polyphenol that presents nonbinding phenolic moieties and reactive ester linkages held at the ZnO surface (**Figure 4**). The myriad competing reaction pathways, such as proton coupled electron transfer involving oxygenated species, make it difficult to elucidate the stabilization mechanism with tannic acid (Supporting Information, Figure S12).^[41–43] However, we can further illuminate the role of the surface binding compared to reactions in the bulk. To test whether the bulk tannic acid was required, the ionic liquid cavity of a working EDLT was removed, the channel flushed with additive free [EMIM][TCB], and a new cavity with a new top electrode and additive free ionic liquid was fitted. The electronic device characteristics did not change upon removing the tannic acid from the liquid (Supporting Information, Figure S9). The experiment shows that the tannic acid forms a surface layer or solid electrolyte interphase (SEI)^[44] on the *a*-ZnO. This layer stays intact after rinsing and provides the

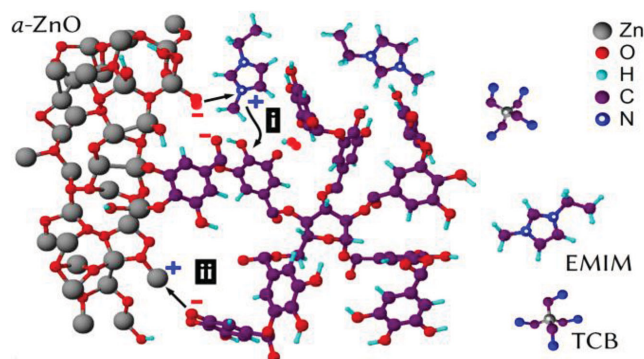


Figure 4. Schematic of the oxide–ionic liquid interface. Cathodic reaction at positive bias where there is (i) the reduction of *a*-ZnO due to loss of oxygen and successive reaction with tannic acid and (ii) the possible attachment of a tannic acid molecule to the surface of *a*-ZnO via unsaturated Zn⁺ sites.

self-healing mechanism. Thus, tannic acid does not have to be resupplied during the device operation as long as the concentration is high enough to rapidly form the interphase after the first bias cycle.

We can further understand the self-healing mechanism by examining voltammetric data available from the current at the gate electrode during operation. The gate current shows specific peaks for reduction and oxidation that can be integrated to yield the charge that is transported in the form of oxygen ions out of and into the *a*-ZnO surface (Supporting Information, Figure S10). Both charges are well balanced around 157 nC and do not depend on the driving frequency, pointing at a good reversibility of the process. Taking the surface area 0.012 cm² of the *a*-ZnO in contact with the ionic liquid, the measured charge translates into a charge density of 8.2×10^{13} cm⁻² or an estimated 15% of the surface oxygen atoms, which is a value typically encountered in EDLT studies on ZnO since the earliest reports.^[14] This sheet charge is moved at the EDL during the hysteresis of 1 V. In order to move 157 nC in the EDLT at 1 V, an effective EDL sheet capacitance of 15.2 μF cm⁻² is required, which is exactly the value measured for the [EMIM][TCB] double layer (Supporting Information, Figure S5). Interestingly, even after stressing the device for 10 min in either the on-state or the off-state, the device's on- and off-currents change by less than 0.5% (Supporting Information, Figure S8). In contrast, the EDLT without additive shows decaying characteristics after a single measurement. Ultimately, if the *a*-ZnO surface etching under bias with tannic acid was not self-limiting and reversible, the 5 nm thick active layer would be destroyed in just a few minutes or a few gate sweep cycles (Supporting Information, Figure S2d). In addition, superoxide dissolved in the ionic liquid can degrade the electrolyte and even the metal electrodes.^[32] The stable operation of the EDLTs with tannic acid shows that a functional layer covering the *a*-ZnO is enough to reduce the amount of harmful superoxide, or other reactive species, in the ionic liquid to a negligible amount. Whether tannic acid frustrates the formation of reactive species or scavenges radicals remains unclear.

At this time, the electrochemical and kinetic mechanisms of tannic acid stabilization cannot be determined with absolute certainty. In general, the electrochemistry of electrolytes in organic interphases remains highly complex and is a very active field of research, especially with respect to the SEI in lithium batteries.^[45] After reduction of the *a*-ZnO surface, oxygen in some form is kept close to the interface and *a*-ZnO_{1-x} can be easily re-oxidized as soon as the bias hits the required electrochemical potential of -1 V (Figure 4). The ex situ XPS measurements after positive and negative bias stress suggest that the ionic liquid itself may be involved in the interfacial kinetic process (Supporting Information, Figure S11). In any practical EDL device, degradation of the IL is unlikely to limit operation due to the small amount of charge (compared to a battery) as long as the degradation products do not harm the components of the device. Even if we cannot measure the particular interface reactions, our results show that the tannic acid plays a dominant role in the modulation of the very thin *a*-ZnO.

While elucidating the interplay between electrochemical reactivity and electronic conduction is complex, the devices are highly reproducible. To demonstrate the potential for

integration, we used two of these Schmitt triggers to build an A/D converter with electric circuit and characteristic (Supporting Information, Figure S13). The device converts a ±4 V input signal into a two bit output while making use of the 1 V hysteresis to enable for noise permissive switching. Looking at the output V_1 of the second Schmitt trigger (ST₁), a quadratic rather than an edge like switching can be seen. This problem is caused by the mismatch between the output bias range with the required input range for a clean switching operation. We expect that a voltage gain bigger than unity, i.e., a smaller hysteresis, can be achieved with other materials systems, e.g., ionic liquids with different electrochemical windows and metal oxide semiconductors with a stoichiometry susceptible to environmental conditions, that is, with a low reduction potential.

It can be concluded that the addition of a multifunctional polyphenol stabilizes EDL transistors of *a*-ZnO by providing reactive oxygen species at the interface and protection of the semiconductor and electrodes from degradation. We believe that these results suggest a great opportunity for electrostatic and electrochemical devices to realize unique building blocks for ubiquitous sensing and processing. Interfaces that employ ion kinetics imply the opportunity to define single devices that have the functionality of a Schmitt trigger and potentially other new nonlinear elements or more complex circuits like impulse generators. New highly parallel circuits that can use devices like Schmitt triggers require fewer components and have increased power efficiency relevant for printable electronics.

Supporting Information

Supporting Information is available from the Wiley Online Library or from the author.

Acknowledgements

This work was provided by the MRSEC Program of the NSF under Award No. DMR-1121053. S.B. was funded by the Deutsche Forschungsgemeinschaft (DFG) Project No. BU 2669/1-1.

Received: February 3, 2015

Revised: March 22, 2015

Published online:

- [1] E. Kandel, *Principles of Neural Science*, 5th ed., McGraw Hill Professional, New York 2013.
- [2] P. Horowitz, W. Hill, *The Art of Electronics*, Cambridge University Press, Cambridge, MA 2006.
- [3] S. Bharitkar, J. M. Mendel, *IEEE Trans. Neural Netw.* 2000, 11, 879.
- [4] J. J. Hopfield, *Proc. Natl. Acad. Sci. USA* 1982, 79, 2554.
- [5] J. Jeong, N. Aetukuri, T. Graf, T. D. Schladt, M. G. Samant, S. S. P. Parkin, *Science* 2013, 339, 1402.
- [6] M. Armand, J.-M. Tarascon, *Nature* 2008, 451, 652.
- [7] V. Augustyn, P. Simon, B. Dunn, *Energy Environ. Sci.* 2014, 7, 1597.
- [8] M. Grätzel, *Nature* 2001, 414, 338.
- [9] W. Lu, A. G. Fadeev, B. Qi, E. Smela, B. R. Mattes, J. Ding, G. M. Spinks, J. Mazurkiewicz, D. Zhou, G. G. Wallace, D. R. MacFarlane, S. A. Forsyth, M. Forsyth, *Science* 2002, 297, 983.
- [10] R. Karnik, C. Duan, K. Castelino, H. Daguji, A. Majumdar, *Nano Lett.* 2007, 7, 547.

- [11] M. Ali, S. Mafe, P. Ramirez, R. Neumann, W. Ensinger, *Langmuir* **2009**, *25*, 11993.
- [12] C. H. Ahn, A. Bhattacharya, M. Di Ventra, J. N. Eckstein, C. D. Frisbie, M. E. Gershenson, A. M. Goldman, I. H. Inoue, J. Mannhart, A. J. Millis, A. F. Morpurgo, D. Natelson, J.-M. Triscone, *Rev. Mod. Phys.* **2006**, *78*, 1185.
- [13] S. H. Kim, K. Hong, W. Xie, K. H. Lee, S. Zhang, T. P. Lodge, C. D. Frisbie, *Adv. Mater.* **2013**, *25*, 1822.
- [14] H. Shimotani, H. Asanuma, A. Tsukazaki, A. Ohtomo, M. Kawasaki, Y. Iwasa, *Appl. Phys. Lett.* **2007**, *91*, 082106.
- [15] J. Ye, M. F. Craciun, M. Koshino, S. Russo, S. Inoue, H. Yuan, H. Shimotani, A. F. Morpurgo, Y. Iwasa, *Proc. Natl. Acad. Sci. USA* **2011**, *108*, 13002.
- [16] S. Z. Bisri, E. Degoli, N. Spallanzani, G. Krishnan, B. J. Kooi, C. Ghica, M. Yarema, W. Heiss, O. Pulci, S. Ossicini, M. A. Loi, *Adv. Mater.* **2014**, *26*, 5639.
- [17] M. Nakano, K. Shibuya, D. Okuyama, T. Hatano, S. Ono, M. Kawasaki, Y. Iwasa, Y. Tokura, *Nature* **2012**, *487*, 459.
- [18] T. A. Petach, M. Lee, R. C. Davis, A. Mehta, D. Goldhaber-Gordon, *Phys. Rev. B* **2014**, *90*, 081108.
- [19] T. D. Schladt, T. Graf, N. B. Aetukuri, M. Li, A. Fantini, X. Jiang, M. G. Samant, S. S. P. Parkin, *ACS Nano* **2013**, *7*, 8074.
- [20] D. Natelson, M. Di Ventra, *MRS Bull.* **2011**, *36*, 914.
- [21] H. Yuan, H. Shimotani, J. Ye, S. Yoon, H. Aliah, A. Tsukazaki, M. Kawasaki, Y. Iwasa, *J. Am. Chem. Soc.* **2010**, *132*, 18402.
- [22] Z. Q. Wang, H. Y. Xu, X. H. Li, H. Yu, Y. C. Liu, X. J. Zhu, *Adv. Funct. Mater.* **2012**, *22*, 2759.
- [23] J. Shi, S. D. Ha, Y. Zhou, F. Schoofs, S. Ramanathan, *Nat. Commun.* **2013**, *4*, 2676.
- [24] M. J. S. Smith, L. Portmann, *IEEE Trans. Circuits Syst.* **1989**, *36*, 42.
- [25] S. Thiemann, S. Sachnov, S. Porscha, P. Wasserscheid, J. Zaumseil, *J. Phys. Chem. C* **2012**, *116*, 13536.
- [26] S. Dasgupta, R. Kruk, N. Mechau, H. Hahn, *ACS Nano* **2011**, *5*, 9628.
- [27] K. Hong, S. H. Kim, K. H. Lee, C. D. Frisbie, *Adv. Mater.* **2013**, *25*, 3413.
- [28] H. Yuan, H. Shimotani, A. Tsukazaki, A. Ohtomo, M. Kawasaki, Y. Iwasa, *Adv. Funct. Mater.* **2009**, *19*, 1046.
- [29] S. Bubel, S. Meyer, F. Kunze, M. L. Chabiny, *Appl. Phys. Lett.* **2013**, *103*, 152102.
- [30] D. Weingarth, I. Czekaj, Z. Fei, A. Foelske-Schmitz, P. J. Dyson, A. Wokaun, R. Kötz, *J. Electrochem. Soc.* **2012**, *159*, H611.
- [31] S. Seki, N. Serizawa, K. Hayamizu, S. Tsuzuki, Y. Umebayashi, K. Takei, H. Miyashiro, *J. Electrochem. Soc.* **2012**, *159*, A967.
- [32] S. Bubel, S. Meyer, M. L. Chabiny, *IEEE Trans. Electron Devices* **2014**, *61*, 1561.
- [33] H. Lee, S. M. Dellatore, W. M. Miller, P. B. Messersmith, *Science* **2007**, *318*, 426.
- [34] T. S. Sileika, D. G. Barrett, R. Zhang, K. H. A. Lau, P. B. Messersmith, *Angew. Chem. Int. Ed.* **2013**, *52*, 10766.
- [35] W. Lin, J. Walter, A. Burger, H. Maid, A. Hirsch, W. Peukert, D. Segets, *Chem. Mater.* **2015**, *27*, 358.
- [36] R. Marczak, F. Werner, J.-F. Gnichwitz, A. Hirsch, D. M. Guldi, W. Peukert, *J. Phys. Chem. C* **2009**, *113*, 4669.
- [37] J. W. Spalanka, P. Gopalan, H. E. Katz, P. G. Evans, *Appl. Phys. Lett.* **2013**, *102*, 041602.
- [38] J. Chen, R. E. Ruther, Y. Tan, L. M. Bishop, R. J. Hamers, *Langmuir* **2012**, *28*, 10437.
- [39] M. Rodenstein, S. Zürcher, S. G. P. Tosatti, N. D. Spencer, *Langmuir* **2010**, *26*, 16211.
- [40] B. P. Fors, J. E. Poelma, M. S. Menyo, M. J. Robb, D. M. Spokoynny, J. W. Kramer, J. H. Waite, C. J. Hawker, *J. Am. Chem. Soc.* **2013**, *135*, 14106.
- [41] D. Neshchadin, S. N. Batchelor, I. Bilkis, G. Gescheidt, *Angew. Chem. Int. Ed.* **2014**, *53*, 13288.
- [42] D. T. Sawyer, T. S. Calderwood, C. L. Johlman, C. L. Wilkins, *J. Org. Chem.* **1985**, *50*, 1409.
- [43] D. T. Sawyer, J. S. Valentine, *Acc. Chem. Res.* **1981**, *14*, 393.
- [44] E. Peled, *J. Electrochem. Soc.* **1979**, *126*, 2047.
- [45] P. Verma, P. Maire, P. Novák, *Electrochimica Acta* **2010**, *55*, 6332.